JACS
JOURNAL OF THE AMERICAN CHEMICAL SOCIETY
Article
pubs.acs.org/JACS

Solubilizing and Stabilizing Proteins in Anhydrous Ionic Liquids through Formation of Protein−Polymer Surfactant Nanoconstructs

Alex P. S. Brogan[†] and Jason P. Hallett*[,†]

[†]Department of Chemical Engineering, Imperial College, London SW7 2AZ, United Kingdom

Supporting Information

ABSTRACT: Nonaqueous biocatalysis is rapidly becoming a desirable tool for chemical and fuel synthesis in both the laboratory and industry. Similarly, ionic liquids are increasingly popular anhydrous reaction media for a number of industrial processes. Consequently, the use of enzymes in ionic liquids as efficient, environment-friendly, commercial biocatalysts is highly attractive. However, issues surrounding the poor solubility and low stability of enzymes in truly anhydrous media remain a significant challenge. Here, we demonstrate for the first time that engineering the surface of a protein to yield protein−polymer surfactant nanoconstructs allows for dissolution of dry protein into dry ionic liquids. Using myoglobin as a model protein, we show that this method can deliver protein molecules with near native structure into both hydrophilic and hydrophobic anhydrous ionic liquids. Remarkably, using temperature-dependent synchrotron radiation circular dichroism spectroscopy to measure half-denaturation temperatures, our results show that protein stability increases by 55 °C in the ionic liquid as compared to aqueous solution, pushing the solution thermal denaturation beyond the boiling point of water. Therefore, the work presented herein could provide a platform for the realization of biocatalysis at high temperatures or in anhydrous solvent systems.

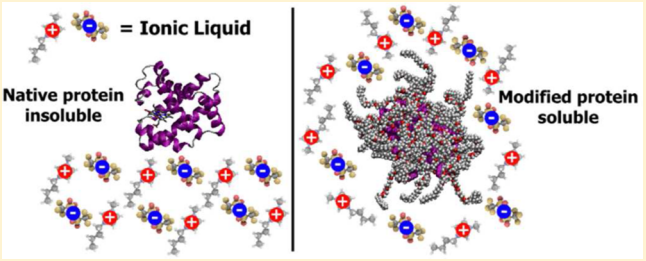

INTRODUCTION

Ionic liquids, organic salts with melting temperatures typically below 100 °C, are becoming increasingly popular as promising solvents for many industrial processes and various other applications.[1,2] The major draw for using ionic liquids is their attractive and highly tunable chemical and physical properties, including high thermal, chemical, and electrochemical stabilities in conjunction with negligible vapor pressures.[2] Recently, the application of ionic liquids in solubilizing biopolymers such as cellulose and lignin has paved the way for the development of new technologies to process lignocellulosic biomass.[3]

While research into the various applications for ionic liquids has progressed, the use of biocatalysts for a number of purposes has also been gaining ground.[4−10] Enzymes can perform many industrially relevant reactions under significantly milder conditions than their chemical counterparts. However, the low stability of proteins in nonaqueous environments has limited their widespread applicability to a select few processes. This creates a conflict between low-temperature aqueous processing, where conditions are optimal for enzyme stability and selectivity, and organic solvent or high-temperature processing, which favor high substrate solubility and vastly improved reaction kinetics, respectively. We aim to resolve this conflict through engineering protein surfaces toward solubility and stability in anhydrous ionic liquid media, providing a platform for high-temperature and nonaqueous bioprocessing.

There have been reported a number of studies concerning proteins and enzymes in ionic liquids.[7−19] Despite this interest, enzymes are poorly soluble in ionic liquids and tend to be highly unstable in the absence of water. A number of strategies are often employed to counteract this, including solid-support immobilization[7,12] or dilution with large amounts of water, which improves enzyme solubility,[7] but at a potential cost to substrate solubility. Alternatively, novel ionic liquids have been developed that are specifically protein/enzyme friendly.[4,6,15,16,18] However, the high costs associated with these bespoke ionic liquids will likely limit commercial application. Despite these advances, the water content and low stability still pose problems with respect to industrial applications, as larger use of expensive proteins is coupled with difficult separation of large amounts of water. Furthermore, recent reviews by Naushad et al.[11] and Gao et al.[7] highlight the frequent contradictions that arise when studying the interactions between proteins and ionic liquids, particularly concerning how the chemical nature of the ions affects protein stability and the role of water in this process. As a result, despite the plethora of enzymes available for processes in ionic liquids, there are to the best of our knowledge no examples of dry biocatalysts solubilized in truly dry ionic liquids. This creates a need to develop new biotechnologies whereby proteins and enzymes can be both solubilized and stabilized in both dry hydrophobic and hydrophilic ionic liquids. This will broaden the scope of biocatalysis in ionic liquids, particularly if water can

Received: December 23, 2015
Published: March 14, 2016

DOI: 10.1021/jacs.5b13425
J. Am. Chem. Soc. 2016, 138, 4494−4501

be excluded and low thermal stability could be overcome, to include the possibility of efficient nonaqueous bioprocessing in these novel solvent media, key examples being the production of biodiesel or hydrophobic pharmaceuticals.

Solvent-free liquid proteins are a new class of hybrid material, where surface modification of proteins and enzymes, by introduction of a polymer−surfactant "organic corona", can allow for a protein-rich biofluid, devoid of any solvent.[20−25] These have recently been shown to preserve the three-dimensional architecture of the biomolecule,[20,21] maintain backbone dynamics as if in water,[22] and retain biological function[23] and enzymatic activity all in the absence of water.[24] Furthermore, these novel fluids significantly increase the thermal stability of the protein/enzyme,[20] and in the case of lipase, enzyme activity was enhanced at temperatures up to 150 °C.[24] Molecular dynamics simulations suggested that the dielectric constant of the organic corona surrounding the protein molecules was similar to polar organic solvents.[25] One potential drawback limiting application of these fluids in their own right is that their viscosity is in the kPa·s range.[23] Mixing these biofluids with ionic liquids would decrease this viscosity, and the enhanced thermal stability of the modified protein would be well-complemented by the high thermal stability and negligible vapor pressure of ionic liquids. The low dielectric of the modified surface should be ideal for solubilizing proteins/enzymes in ionic liquids and ought to provide protection from the ions, which can be adept at disrupting hydrogen-bonded structures.[26]

Here, we demonstrate our surface modification technique with a model myoglobin system in the presence of several ionic liquids. Specifically, we have synthesized protein−polymer surfactant nanoconstructs, yielding a protein-rich biofluid that, to the best of our knowledge, is the first example of a highly soluble dry protein in both hydrophilic and hydrophobic ionic liquids. Thermal stability of the modified myoglobin increases by 55 °C in ionic liquid solution as compared to aqueous solutions, demonstrating a positive impact of the ionic liquid on the modified protein's stability. Our results demonstrate that engineering the surface of a protein favorably alters the manner in which it interacts with ionic liquids. This could be a general pathway to the realization of ionic liquid soluble proteins and enzymes with high thermal stability, leading to the development of biocatalysts for myriad nonaqueous bioprocessing opportunities.

MATERIALS AND METHODS

Preparation of Protein−Polymer Surfactant Biofluids. Protein−polymer surfactant nanoconstructs were prepared using established methods.[23] Briefly, *N*,*N*′-bis(2-aminoethyl)-1,3-propanediamine (Sigma) was coupled to the aspartic and glutamic acid residues of equine skeletal muscle myoglobin (Mb) (Sigma) via carbodiimide activation. The resultant C−Mb solution was dialyzed against deionized water for 48 h and filtered using a 0.22 μm syringe filter. This solution was then added to a neutralized solution of the surfactant ethylene glycol ethoxylate lauryl ether (S) ($M_n \sim 690$ g·mol^{-1}; Sigma) and stirred for 12 h to produce the [C−Mb][S] nanoconstruct. This was dialyzed against deionized water for 48 h to remove unbound S and then freeze-dried to yield a light brown powder that formed the solvent-free biofluid after thermal annealing.

Synthesis of Ionic Liquids. For the ionic liquid synthesis, all reagents were bought from Sigma, dried over P_2O_5, and purified further as necessary. 1-Butyl-1-methylpyrrolidinium chloride was synthesized as follows. Freshly distilled *N*-methylpyrrolidine (311.65 g, 3.66 mol) was added dropwise to a mixture of freshly distilled 1-chlorobutane (309.18 g, 3.33 mol) and ethyl acetate (300 mL). The reaction was heated for 3 days at 75 °C and upon completion the mixture was placed in a freezer overnight to encourage precipitation and then the solvent was removed via Schlenk techniques. The precipitate was washed with ethyl acetate, recrystallized in acetonitrile, and dried in vacuo to yield 1-butyl-1-methylpyrrolidinium chloride (356.66 g, 60.3%) as a white crystalline solid.

1-Butyl-1-methylpyrrolidinium bis(trifluoromethylsulfonyl)imide ([bmpy][NTf$_2$]) was synthesized as follows. A mixture of 1-butyl-1-methylpyrrolidinium chloride (33.78 g, 0.19 mol) and dichloromethane (50 mL) was added to lithium bis(trifluoromethylsulfonyl)-imide (60.29 g, 0.21 mol) and stirred vigorously at room temperature for 24 h. The mixture was filtered and washed repeatedly with deionized water (10 × 100 mL) until no chloride traces remained (tested with silver nitrate solution). The ionic liquid in dichloromethane was purified through a short alumina column topped with a thin layer of activated charcoal (ca. < 5 mm). The solvent was then removed in vacuo (24 h), giving [bmpy][NTf$_2$] (71.29 g, 89%) as a colorless viscous liquid.

Similarly, 1-butyl-1-methylpyrrolidinium trifluoromethanesulfonate ([bmpy][OTf]) was synthesized as follows. A mixture of 1-butyl-1-methylpyrrolidinium chloride (67.88 g, 0.38 mol) and acetone (50 mL) was added to sodium trifluoromethanesulfonate (71.92 g 0.42 mol) and the reaction was stirred for 48 h at room temperature. The resulting organic phase was filtered and washed with water until chloride tests proved negative (silver nitrate test). The solvent was then removed via rotary evaporation and the ionic liquid was passed through a short alumina column topped with a layer of activated charcoal (ca. < 5 mm). The remaining liquid was dried in vacuo (24 h), giving [bmpy][OTf] (72.15 g, 65.18%) as a colorless viscous liquid.

Spectroscopic Methods. UV/vis spectroscopy was performed on a Shimadzu UV2600 fitted with a Peltier controlled heating environment. Aqueous solutions of Mb, C−Mb, and [C−Mb][S] were measured in 10 mm quartz cuvettes at 25 °C. Solvent-free [C−Mb][S] and [C−Mb][S] solutions were measured in a 0.01 mm two-part quartz cell at 25 °C. All spectra were recorded using the "fast" setting with automatic sampling enabled.

Synchrotron radiation circular dichroism (SRCD) spectroscopy was performed at Diamond Light Source on beamline B23 using module A, fitted with a custom Linkam stage for temperature control. Spectra were collected between 260 and 180 nm with an integration time of 2 s and data interval of 1 nm. Aqueous solutions (0.1−0.3 mg·mL^{-1}, 10 mM pH 6.8 phosphate buffer) of Mb, C−Mb, and [C−Mb][S] were run in 1 mm quartz cuvettes. Solvent-free liquid [C−Mb][S] samples were measured as thin films cast between quartz plates. For [C−Mb][S] in ionic liquid, samples were prepared as 50% solutions, to minimize solvent absorption, and cast as films between quartz plates. Subsequent spectra of both solvent-free and ionic liquid solutions of [C−Mb][S] were normalized to intensity recorded at 222 nm of samples in 0.01 mm quartz cells (protein absorbance was too high to measure spectra across the complete range in 0.01 mm quartz cells). This was to ensure that mean residue ellipticity could be reasonably calculated. Spectra were deconvoluted to estimate secondary structure content with the DichroWeb service, using the SP175 data set, and the CDSSTR analysis program.[27−29] Errors presented for the secondary structure for the solvent-free and ionic liquid solutions account for potential variation in film thickness between samples. Thermal denaturation of [C−Mb][S] samples (aqueous, solvent-free, and ionic liquid) were performed using the above parameters. Solvent-free and ionic liquid samples were measured in the temperature range 0−210 °C with spectra recorded every 10 °C. Aqueous samples were measured in the temperature range 25−95 °C with spectra recorded every 5 °C. The heating rate was set to 100 °C·min^{-1}, and samples were equilibrated for 2 min before spectra were recorded.

FTIR spectroscopy was measured using a PerkinElmer Spectrum 100 fitted with a Specac attenuated total reflection (ATR) accessory. Spectra were recorded as accumulations of eight scans with a bandwidth of 2 cm^{-1}.

DOI: 10.1021/jacs.5b13425
J. Am. Chem. Soc. 2016, 138, 4494−4501

RESULTS AND DISCUSSION

Conjugation of myoglobin (Mb) cationized with *N*,*N*′-bis(2-aminoethyl)-1,3-propanediamine (C−Mb) with the surfactant glycolic acid ethoxylate lauryl ether (S) yielded a protein−polymer surfactant construct [C−Mb][S] with a stoichiometry of 84 surfactant molecules per protein (SI Figure 1, Supporting Information). Upon dehydration and thermal annealing, this formed a dark brown-red, protein rich, solvent-free biofluid with a melting temperature of 27 °C (amorphous-solid to liquid transition, SI Figure 2, Supporting Information). The solvent-free liquid was soluble in water and polar organic solvents such as ethanol. Importantly, the protein−polymer surfactant conjugates were highly miscible (solubility of >50 wt %) with both hydrophilic ([bmpy][OTf]) and hydrophobic ([bmpy][NTf_2]) ionic liquids (Figure 1). The homogeneity of modified

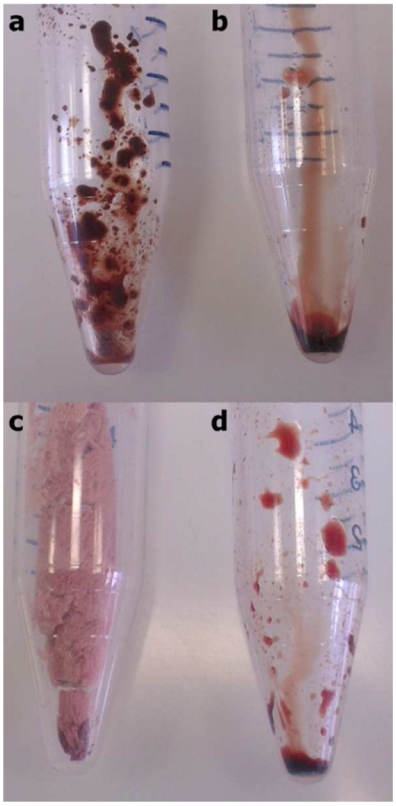

Figure 1. Images showing 50 wt % mixtures of lyophilized Mb in [bmpy][OTf] (a), [C−Mb][S] in [bmpy][OTf] (b), Mb in [bmpy][NTf_2] (c), and [C−Mb][S] in [bmpy][NTf_2] (d). Samples were prepared by freeze-drying aqueous solutions of protein and ionic liquid.

myoglobin−ionic liquid mixtures was in stark contrast to the heterogeneous mixture of unmodified Mb and [bmpy][OTf] (maximum solubility of 5.6 wt %) and the complete lack of mixing of unmodified Mb with [bmpy][NTf_2] (solubility of <0.3 wt %, Figure 1). Karl Fischer titration indicated water contents of 0.2 and 0.3 wt % for the [bmpy][OTf] and [bmpy][NTf_2] mixtures, respectively. These values correspond to 12−19 water molecules per [C−Mb][S] construct. This is significantly fewer than the 526 water molecules to cover the accessible surface area of Mb and fewer than the 60 required as a "lower limit" for protein motion.[20] As a result, although there is residual water present, the systems can be affectively thought of as being water-free.

This demonstrates that modifying the protein surface to form the solvent-free biofluids increased the solubility of the dry protein in anhydrous ionic liquids, yielding the first example (to the best of our knowledge at the time of writing) of a soluble protein solution in the near total absence of water. Overcoming these solubility issues minimized protein aggregation in the hydrophilic ionic liquid and allowed for the introduction of protein into the more hydrophobic [NTf_2] system, which has not previously been demonstrated.

To assess the impact of the ionic liquids on the three-dimensional global conformation of the modified protein, the states of the secondary and tertiary structures of [C−Mb][S] were determined using a number of spectroscopic measurements. UV/vis spectroscopy showed Soret bands at 412 and 413 nm and Q bands at 529 and 535 nm, for [C−Mb][S] in [bmpy][OTf] and [bmpy][NTf_2], respectively (Figure 2a). This corresponds well with the Soret and Q absorptions of [C−Mb][S] in the solvent-free liquid state (413, 535 nm) and in aqueous solutions (409, 530 nm) (Figure 2a). This indicates that in aqueous and ionic liquid solutions and in the solvent-free liquid state, the prosthetic heme group of Mb is still bound to the protein. Furthermore, the topology of the binding pocket remains unchanged in the different environments. Attenuated total reflectance (ATR) FTIR spectroscopy showed amide I and amide II bands at 1655 and 1545 cm^{-1}, respectively, for [C−Mb][S] in both ionic liquids and the solvent-free state, indicative of a highly conserved α-helical structure (Figure 2b). This is in broad agreement with the UV/vis spectra, demonstrating that the global conformation of Mb is maintained even in the anhydrous ionic liquids. The presence of highly conserved Mb structure was confirmed using synchrotron radiation circular dichroism (SRCD), which showed negative peaks at 222 and 208 nm with a positive peak at 195 nm for [C−Mb][S] in the ionic liquid, solvent-free, and aqueous environments (Figure 2c). These peak positions are highly indicative of a predominantly α-helical structure for [C−Mb][S], agreeing well with the ATR-FTIR spectra. The SRCD spectra revealed quite significant changes in the structure content of [C−Mb][S] between the aqueous and nonaqueous environments. Dehydration of aqueous [C−Mb][S] nanoconjugates to yield the solvent-free liquid caused a reversal in the ratio of the negative features at 208 and 222 nm, where the increase in the 222 nm intensity suggested an increase in α-helical structure. This was confirmed through deconvolution of the spectra using the DichroWeb service,[27−29] which showed that there was indeed a moderate increase in α-helix content from 51% to 54% upon dehydration (Table 1).

Meanwhile, the SRCD spectra of [C−Mb][S] in ionic liquids showed an increase in the absolute intensities of all the spectral features, particularly the positive feature at 195 nm (Figure 1c), with the increase in secondary structure most apparent in [bmpy][OTf]. Deconvolution suggested that moving from the solvent-free liquid state to [bmpy][OTf] and [bmpy][NTf_2] caused an increase in the α-helix content of [C−Mb][S] to 69% and 61% (from 51%), respectively (Table 1).

Increasing α-helix content was concomitant with a decrease in the unordered content, suggesting that the ionic liquids were inducing α-helix formation and therefore increasing structure, relative to both the aqueous and solvent-free protein states. It must be noted that the structure of aqueous [C−Mb][S] represents a destabilized form of Mb (51% α-helix content compared to 72% α-helix content for native Mb; SI Figure 3, SI Table 1, Supporting Information) due to the cationization

DOI: 10.1021/jacs.5b13425
J. Am. Chem. Soc. 2016, 138, 4494−4501

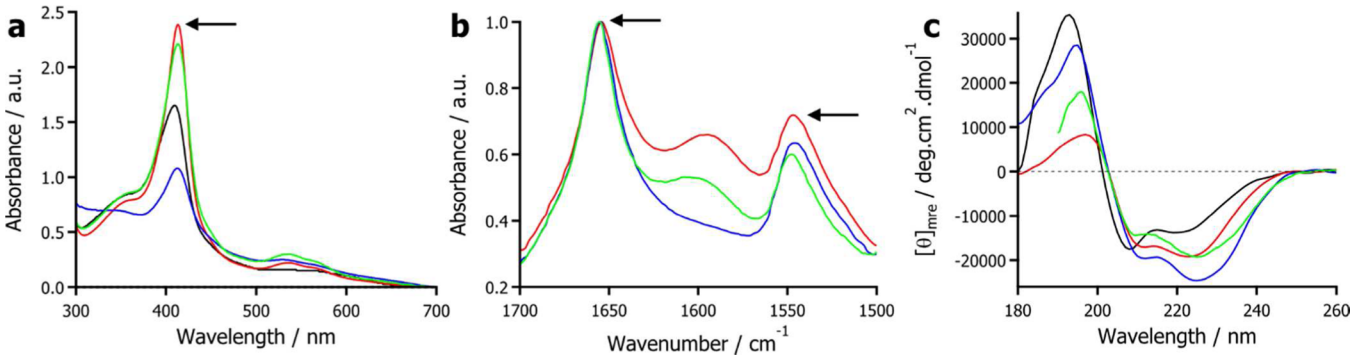

Figure 2. UV/vis spectra showing the Soret band region (a), ATR-FTIR spectra showing the amide I and II region (b), and SRCD spectra showing the far-UV region (c) for aqueous [C−Mb][S] (black), solvent-free [C−Mb][S] (red), [C−Mb][S] in [bmpy][OTf] (blue), and [C−Mb][S] in [bmpy][NTf_2] (green). Ionic liquid solutions were prepared at a [C−Mb][S] concentration of 50 wt %, and aqueous solutions were prepared with 10 mM phosphate buffer (pH 6.8). All spectra we recorded at 25 °C. ATR-FTIR spectrum was not recorded for aqueous solution due to water interference.

Table 1. Estimated Secondary Structure Content As Determined by SRCD Spectra in Figure 2c Using the DichroWeb Service[27−29]

[C−Mb][S]	α-helix/%	β-sheet/%	turns/%	unordered/%	NRMSD
aqueous	51	11	11	27	0.009
solvent-free	54 ± 6	10 ± 1	12 ± 2	24 ± 5	0.004
[bmpy][OTf]	69 ± 6	6 ± 3	10 ± 2	15 ± 3	0.005
[bmpy][NTf_2]	61	8	11	20	0.008

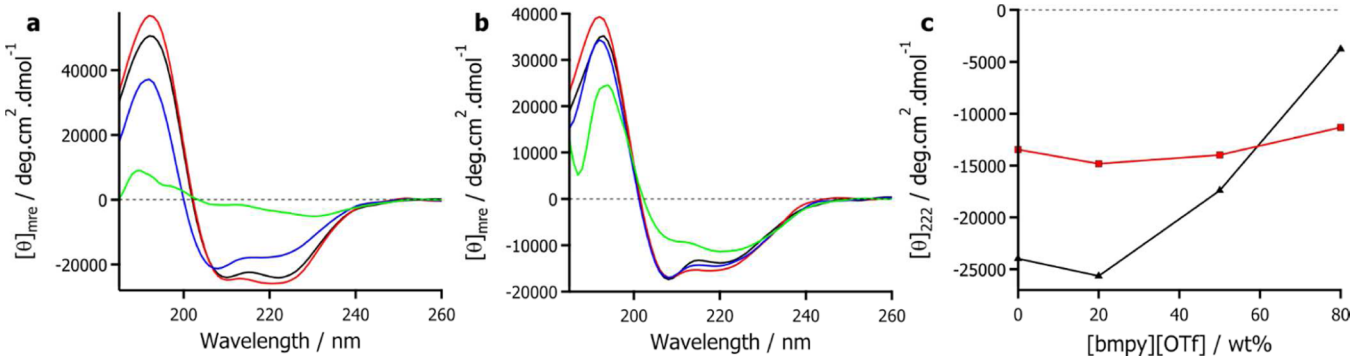

Figure 3. SRCD spectra of the far-UV region for aqueous solutions of Mb (a) and [C−Mb][S] (b) showing response to [bmpy][OTf] concentrations of 0% (black), 20% (red), 50% (blue), and 80% (green). (c) Plots of mean residue ellipticity at 222 nm against [bmpy][OTf] concentration for aqueous solutions of Mb (black triangles) and [C−Mb][S] (red squares).

process causing a destabilization of the native myoglobin state, such that a shift to a molten globule state occurs as described previously.[20]

Therefore, the significant increase in secondary structure observed in the anhydrous ionic liquid solution could be justified as an ionic-liquid-induced re-formation of the native Mb global fold, as opposed to forming a new, non-native structure. This structuration of the sections of unordered backbone of [C−Mb][S] suggests that the ionic liquids act as helix-enhancing solvents, restoring the structure of the modified protein toward that exhibited in the unmodified state, consistent with polar organic environments such as those containing fluoro alcohols.[30−32] Furthermore, these observations suggest that the OTf^- anion was able to interact with the biomolecule with greater effect than NTf_2^-, as may be expected given the greater hydrogen bond basicity (β) of OTf^-.[33] Additionally, from a Hofmeister perspective, OTf^- should provide greater stability than NTf_2^-, and here that trend remains.[19] However, it is worth noting that according to the overall Hofmeister series, both of these anions ought to be destabilizing. In the anhydrous solutions, however, we see significant stabilization of the protein fold, potentially highlighting the limitations of the series at high ionic liquid concentrations (and here in the anhydrous ionic liquid).[11] The interactions involved are therefore more complex, and given the presence of the surfactant coronal layer, it is likely that the relative molecular bulk and lower charge density of NTf_2^- as compared to OTf^- may also affect interactions with the protein surface. It is often accepted that anions with high β values and nucleophilicities interact strongly with protein surfaces and destabilize them.[7,11] As a result, it is often assumed that proteins are stabilized by an absence of these interactions. However, the results presented here indicate a more subtle picture where favorable interactions between ionic liquid anions and proteins can arise and promote structural integrity.

It is interesting to note that protein structuration only occurred under anhydrous conditions. SRCD spectra of aqueous solutions of Mb showed structure decreasing with

DOI: 10.1021/jacs.5b13425
J. Am. Chem. Soc. 2016, 138, 4494−4501

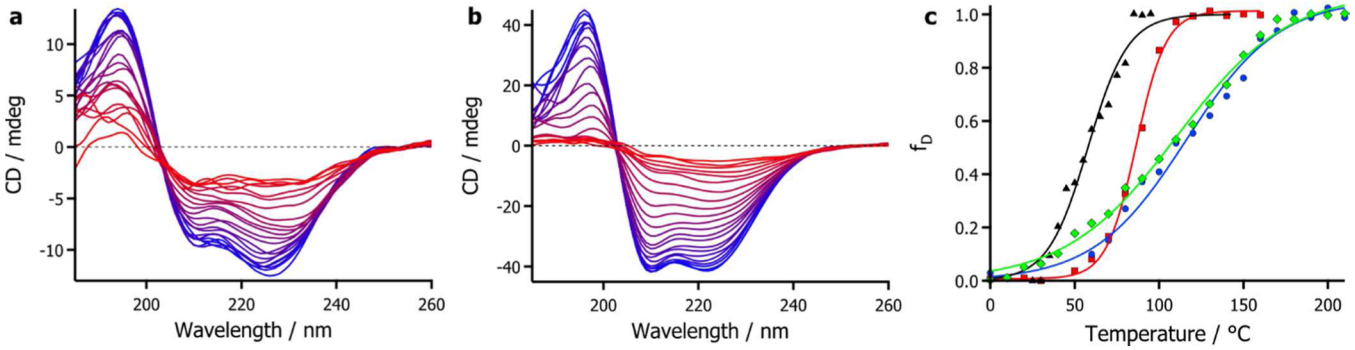

Figure 4. Temperature-dependent far-UV SRCD spectra showing thermal denaturation of [C−Mb][S] (50% solutions) in [bmpy][OTf] (a) and [bmpy][NTf_2] (b) from 0 °C (blue) to 210 °C (red) at intervals of 10 °C. (c) Plot of fraction denatured as calculated from SRCD spectra for aqueous [C−Mb][S] (black triangles), solvent-free [C−Mb][S] (red squares), [C−Mb][S] in [bmpy][OTf] (blue circles), and [C−Mb][S] in [bmpy][NTf_2] (green diamonds). Data were fitted with sigmoid functions (solid lines) in accordance with a two-state model of denaturation.

increasing concentration of [bmpy][OTf] (Figure 3a), in line with observations of proteins in organic solvents, where low levels of water can often be destabilizing.[34,35] Although there was no increase in structuration with ionic liquid concentration, modification of the protein did provide some protection against these effects, as the structuration of [C−Mb][S] only decreased at high (80%) ionic liquid concentrations (Figure 3b). This becomes more apparent using a plot of the mean residue ellipticity at 222 nm as an indication of secondary structure (Figure 3c). Although [C−Mb][S] is in the aforementioned destabilized molten globule state, more structure remained at high ionic liquid concentration than for the native protein, demonstrating that the surfactant corona around the modified protein provides protection from the otherwise denaturing effects of the ionic liquid. This moderate level of structure preservation observed for [C−Mb][S] in response to ionic liquid concentration was only valid for nonacidic anions; these experiments repeated with the highly acidic ionic liquid [N_{2220}][HSO_4] yielded no apparent benefit of protein modification with respect to secondary structure protection (SI Figure 4, Supporting Information). In these experiments, low concentrations (<10%) of the ionic liquid destabilized both Mb and [C−Mb][S], showing that the organic corona could not offer any protection against the highly interacting HSO_4^- anion, and low pH, in aqueous conditions.

In light of the increase in secondary structure observed for [C−Mb][S] in [bmpy][OTf] and [bmpy][NTf_2], temperature-dependent SRCD spectra were recorded to assess whether this translated to an increase in thermal stability of the modified protein when solubilized in the ionic liquids (Figure 4) relative to the solvent-free state. Increasing the temperature from 0 to 210 °C saw progressive reductions of the intensity of the spectral features at 222, 208, and 195 nm, indicative of thermal denaturation occurring over a large temperature range (Figure 4a,b). This showed that in pure ionic liquids, [C−Mb][S] was dynamically free enough to sample the conformations required to unfold, even at low (<30 °C) temperatures. Furthermore, the presence of an isodichroic point at 204 nm suggests that the denaturation process occurred via a two-state transition from a native state to a denatured state. With this in mind, the SRCD data was used to construct a plot of fraction denatured (f_D) against temperature (Figure 4c). In neat [bmpy][OTf] and [bmpy][NTf_2], [C−Mb][S] had half-denaturation temperatures (T_m) of 113 and 108 °C, respectively (Table 2). This was an increase in thermal stability of 27/22 °C from the solvent-free liquid state [T_m = 86 °C, Figure 4c, SI Figure 5 (Supporting Information), Table 2] and 55/50 °C from aqueous [C−Mb][S] [T_m = 58 °C, Figure 4c, SI Figure 6 (Supporting Information), Table 2]. The former results are in agreement with previous findings[20,21,24] that dehydration to form the solvent-free liquid increased the thermal stability of the protein. However, the latter results reveal that even generic ionic liquids can further enhance this stabilization, despite an increase in translational entropy offered by the lower protein concentration, mirroring the observed increases in secondary structure (Figure 2c, Table 1). This indicates that the ionic liquids are interacting favorably with the protein, causing an increase in stability that is a direct response to the increase in secondary structure. Concurrently, stabilization was marginally lower when the anion was NTf_2^-, signifying that the hydrophobicity of this ion may offset some of the stability gains conferred by the surfactant corona. Alternatively, in agreement with the increase in secondary structure seen with the OTf^- anion, the strength of interaction between the anion and protein may be playing a role. Thermal stability in the ionic liquids appears to be associated with a decrease in the cooperativity of the unfolding, as evidenced through a shallowing of the slope of the unfolding curve (Figure 4c), indicating that the ionic-liquid-induced structuration of [C−Mb][S] came at a cost to protein flexibility, exacerbating the relatively noncooperative unfolding of the molten-globule-like structure. This suggests that the observed increase in structure was not a return to the compact globule associated with Mb, but rather that the ionic liquid may cause a shift in the mechanism of unfolding toward multistate denaturation. Unfortunately, the resolution of CD spectroscopy is not sufficient to establish this absolutely; therefore, a more detailed atomistic approach is necessary to confirm this hypothesis.

Table 2. Thermodynamic Parameters for the Thermal Denaturation of [C−Mb][S] in Aqueous Solution, the Solvent-Free State, and in Ionic Liquid[a]

[C−Mb][S]	T_m/°C	ΔS_m/J·K^{-1}·mol^{-1}	ΔH_m/kJ·mol^{-1}
aqueous	58 ± 1	171 ± 17	9.9 ± 0.2
solvent-free	86.4 ± 0.6	304 ± 30	25.7 ± 0.3
[bmpy][OTf]	113 ± 4	89 ± 6	9.8 ± 0.1
[bmpy][NTf_2]	108 ± 2	86 ± 4	9.0 ± 0.1

[a]Values calculated using a two-state model applied to temperature-dependent SRCD spectra (see the Supplementary Information for further details).

DOI: 10.1021/jacs.5b13425
J. Am. Chem. Soc. 2016, 138, 4494−4501

Using a two-state model of denaturation, justified by the existence of an isodichroic point at 204 nm in the SRCD data, we extracted values for the entropy (ΔS_m) and enthalpy (ΔH_m) of denaturation from plots of f_D (see the Supporting Information for details). For [C−Mb][S] in [bmpy][OTf], ΔS_m and ΔH_m were calculated as 89 J·K^{-1}·mol^{-1} and 9.8 kJ·mol^{-1}, and in [bmpy][NTf$_2$] as 86 J·K^{-1}·mol^{-1} and 9.0 kJ·mol^{-1} (Table 2, SI Figure 7, Supporting Information). Values of ΔS_m and ΔH_m calculated for [C−Mb][S] in water were 170 J·K^{-1}·mol^{-1} and 9.9 kJ·mol^{-1}, respectively (Table 2, SI Figure 8, Supporting Information). Given the negligible change in enthalpy between the ionic liquid and aqueous solutions, the observed stabilization of the protein in the ionic liquids was entirely due to a reduction in entropy. This is in broad agreement with the decrease in cooperativity of the transition and serves as evidence that increased protein stability in the ionic liquid was not a result of any increase in favorable interactions within the protein.

The observed ΔS_m for the OTf^- and NTf_2^- ionic liquids were comparable, despite differences in β values and expected specific ion effects, suggesting that entropic stabilization was key across both systems. However, ΔH_m was marginally lower in the NTf_2^- ionic liquid, indicating that the slightly lower stability of [C−Mb][S] in the more hydrophobic environment was predominately due to a small change in enthalpy.

We rationalize this as the more hydrophobic nature of [bmpy][NTf$_2$] stabilizing the unfolded state of the protein more than [bmpy][OTf], reducing the enthalpic cost of denaturation. By contrast, ΔS_m and ΔH_m for solvent-free [C−Mb][S] were calculated at 304 J·K^{-1}·mol^{-1} and 25.7 kJ·mol^{-1}, respectively (Table 2, SI Figure 9, Supporting Information), showing that in the absence of any solvent the situation is much more complex. Any enthalpic gains from the increased strength of stabilizing interactions within the protein in the absence of solvent were offset by the conformational freedom of the protein within the surfactant-coronal layer. Since myoglobin has a propensity to occupy a molten globule state, engineering the surface in the manner reported herein causes such a change.[20] It is therefore plausible that increased stability upon transferring the protein from an aqueous phase to an ionic liquid phase may be a consequence of this unusual molten globule structure. However, given that previous results indicate that modifying more robust enzymes such as lysozyme or lipase give greater stabilities than the myoglobin system,[21,24] we believe that the ionic liquid stability will be transferable.

In light of possible changes to the unfolding pathway of [C−Mb][S] in the ionic liquid, the reversibility of denaturation was probed using UV/vis spectroscopy (Figure 5). Equilibrating the [C−Mb][S]/[bmpy][OTf] mixture at 95 °C caused a reduction and broadening in the Soret absorbance concomitant with a blue shift in the peak position from 412 to 393 nm (Figure 5a). This indicates a change in the global conformation of myoglobin consistent with partial denaturation. On cooling to 25 °C, the Soret band sharpened and returned to 412 nm with a >90% recovery in intensity. This demonstrates that in the ionic liquid solution, the protein was able to recover the structure lost at high temperatures, consistent with the high thermal stability observed using SRCD (Figure 4). Furthermore, once in a (partially) denatured form, the protein was able to refold to its previous structure. This was repeated with [bmpy][NTf$_2$] as the ionic liquid (Figure 5b). On heating to 95 °C the Soret band once again reduced in intensity and underwent a blue shift from 413 to 408 nm, indicating a change

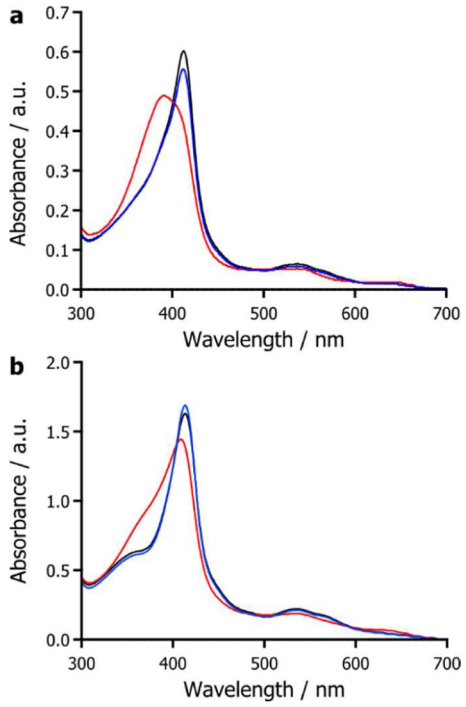

Figure 5. UV/vis spectroscopy showing [C−Mb][S] in [bmpy][OTf] (a) and [bmpy][NTf$_2$] (b) at 25 °C (black), after incubation at 95 °C (red) and after cooling back down to 25 °C (blue).

to a more denatured structure, albeit slightly more structured than for [C−Mb][S] in [bmpy][OTf]. Upon cooling to 25 °C, there was again a >90% recovery in the Soret intensity, with the peak position returning to 413 nm, indicating structural recovery in the more hydrophobic ionic liquid. These results are in broad agreement with the SRCD data (Figure 4), demonstrating further that [C−Mb][S] has a high thermal stability in ionic liquids and also that the protein is able to refold from a partially denatured state, in both hydrophilic and hydrophobic ionic liquids. This indicated that despite apparent constriction of the protein in the ionic liquids, as evidenced through the small changes in entropy on denaturation, the protein was still able to sample multiple conformations. Therefore, introduction of a coronal layer provides an interface between the protein surface (both native and denatured) and the ionic liquid, allowing for reversible perturbations in global conformation.

■ CONCLUSIONS

Here, we have demonstrated that surface modification of myoglobin, yielding the solvent-free liquid [C−Mb][S], can be used as a platform to successfully solubilize the protein in both hydrophilic and hydrophobic ionic liquids in the absence of water. Spectroscopic methods (UV/vis, SRCD, FTIR) establish that there has been preservation of the secondary and tertiary structures of the protein, with significant structuration of the protein occurring, particularly in the case of [bmpy][OTf]. This signifies that the ionic liquids are an environment highly conducive toward protein stability, and SRCD measurements confirmed that thermal denaturation occurs over a large temperature range. With a denaturation temperature of 113 °C, some 55 °C higher than that in aqueous solutions, we were able to show that modification of myoglobin not only increased solubility in ionic liquids but allowed for a thermal

DOI: 10.1021/jacs.5b13425
J. Am. Chem. Soc. 2016, 138, 4494−4501

stability surpassing what is possible in water. Thermally induced unfolding and subsequent refolding from 95 °C reinforced that the modified protein was robust toward both the ionic liquid medium and thermal stresses. Using a two-state model of denaturation, the increase in thermal stability from the aqueous to the ionic liquid phase appeared to be the result of decreasing entropy of denaturation. We attribute this to subtle solvent-induced changes in the unfolding mechanism, resulting in lower cooperativity of the transition. This is possibly a direct manifestation of a putative molten globule state of [C−Mb][S], although a more complex set of interactions between the ionic liquid and the protein is also possible. The net result of high thermal stability, with reversible unfolding, indicates that the forces stabilizing protein structure, as well dynamic flexibility, can be well-maintained in, and even enhanced by, ionic liquids.

We have shown that through modification of the surface of myoglobin, it is possible to greatly increase the solubility of the dry protein in dry ionic liquids. The resulting protein-rich fluids have highly conserved protein architecture and high thermal stability. The synthetic procedure has previously been shown to be very versatile, with solvent-free biofluids of a number of proteins,[21,23] enzymes,[24,36] and viruses[37] having been reported. In combination with the results presented herein, we propose that this biotechnology could provide a platform for the realization of highly soluble ionic liquid and temperature-stable enzymes, providing pathways for improved biocatalysis in ionic liquids and generally homogeneous biocatalysis in anhydrous systems. As a result, we have begun a research program investigating the stability and function of industrially relevant enzymes, such as lipase, β-glucosidase, xylanase, and laccase, in ionic liquids.

■ ASSOCIATED CONTENT

Supporting Information

The Supporting Information is available free of charge on the ACS Publications website at DOI: 10.1021/jacs.5b13425.

Thermal analysis, aqueous SRCD spectra, thermal denaturation plots, and calculated free energy plots (PDF)

■ AUTHOR INFORMATION

Corresponding Author

*j.hallet@imperial.ac.uk.

Author Contributions

The manuscript was written through contributions of all authors. All authors have given approval to the final version of the manuscript.

Notes

The authors declare no competing financial interest.

■ ACKNOWLEDGMENTS

We thank EPSRC (Frontier Engineering Grant EP/K038648/1) for financial support. We also thank Dr. Giuliano Siligardi and Dr. Rohanah Hussain at Diamond Light Source for access to the B23 beamline, Paul Joseph Corbett for ionic liquid synthesis, and Patricia Carry for access to FTIR and DSC.

■ REFERENCES

(1) Smiglak, M.; Pringle, J. M.; Lu, X.; Han, L.; Zhang, S.; Gao, H.; MacFarlane, D. R.; Rogers, R. D. *Chem. Commun.* **2014**, *50*, 9228−9250.

(2) Hallett, J. P.; Welton, T. *Chem. Rev.* **2011**, *111*, 3508−3576.

(3) Brandt, A.; Gräsvik, J.; Hallett, J. P.; Welton, T. *Green Chem.* **2013**, *15*, 550−583.

(4) Bi, Y.-H.; Duan, Z.-Q.; Li, X.-Q.; Wang, Z.-Y.; Zhao, X.-R. *J. Agric. Food Chem.* **2015**, *63*, 1558−1561.

(5) Bokinsky, G.; Peralta-Yahya, P. P.; George, A.; Holmes, B. M.; Steen, E. J.; Dietrich, J.; Lee, T. S.; Tullman-Ercek, D.; Voigt, C. A.; Simmons, B. A.; Keasling, J. D. *Proc. Natl. Acad. Sci. U. S. A.* **2011**, *108*, 19949−19954.

(6) Deive, F. J.; Ruivo, D.; Rodrigues, J. V.; Gomes, C. M.; Sanromán, M. Á.; Rebelo, L. P. N.; Esperança, J. M. S. S.; Rodríguez, A. *RSC Adv.* **2015**, *5*, 3386−3389.

(7) Gao, W.-W.; Zhang, F.-X.; Zhang, G.-X.; Zhou, C.-H. *Biochem. Eng. J.* **2015**, *99*, 67−84.

(8) Huang, Z.-L.; Yang, T.-X.; Huang, J.-Z.; Yang, Z. *BioEnergy Res.* **2014**, *7*, 1519−1528.

(9) Guncheva, M.; Paunova, K.; Yancheva, D.; Svinyarov, I.; Bogdanov, M. *J. Mol. Catal. B: Enzym.* **2015**, *117*, 62−68.

(10) van Rantwijk, F.; Sheldon, R. A. *Chem. Rev.* **2007**, *107*, 2757−2785.

(11) Naushad, M.; ALOthman, Z. A.; Khan, A. B.; Ali, M. *Int. J. Biol. Macromol.* **2012**, *51*, 555−560.

(12) Lozano, P.; Bernal, J. M.; Garcia-Verdugo, E.; Sánchez-Gomez, G.; Vaultier, M.; Burguete, I.; Luis, S. V. *Green Chem.* **2015**, *17*, 3706−3717.

(13) Kumar, A.; Venkatesu, P. *Process Biochem.* **2014**, *49*, 2158−2169.

(14) Reddy, P. M.; Umapathi, R.; Venkatesu, P. *Phys. Chem. Chem. Phys.* **2015**, *17*, 184−190.

(15) Fujita, K.; MacFarlane, D. R.; Forsyth, M. *Chem. Commun.* **2005**, *70*, 4804−4806.

(16) Gorke, J.; Srienc, F.; Kazlauskas, R. *Biotechnol. Bioprocess Eng.* **2010**, *15*, 40−53.

(17) Moniruzzaman, M.; Nakashima, K.; Kamiya, N.; Goto, M. *Biochem. Eng. J.* **2010**, *48*, 295−314.

(18) Moniruzzaman, M.; Kamiya, N.; Goto, M. *Org. Biomol. Chem.* **2010**, *8*, 2887−2899.

(19) Weingärtner, H.; Cabrele, C.; Herrmann, C. *Phys. Chem. Chem. Phys.* **2012**, *14*, 415−426.

(20) Brogan, A. P. S.; Siligardi, G.; Hussain, R.; Perriman, A. W.; Mann, S. *Chem. Sci.* **2012**, *3*, 1839−1846.

(21) Brogan, A. P. S.; Sharma, K. P.; Perriman, A. W.; Mann, S. *J. Phys. Chem. B* **2013**, *117*, 8400−8407.

(22) Gallat, F.-X.; Brogan, A. P. S.; Fichou, Y.; McGrath, N.; Moulin, M.; Härtlein, M.; Combet, J.; Wuttke, J.; Mann, S.; Zaccai, G.; Jackson, C. J.; Perriman, A. W.; Weik, M. *J. Am. Chem. Soc.* **2012**, *134*, 13168−13171.

(23) Perriman, A. W.; Brogan, A. P. S.; Cölfen, H.; Tsoureas, N.; Owen, G. R.; Mann, S. *Nat. Chem.* **2010**, *2*, 622−626.

(24) Brogan, A. P. S.; Sharma, K. P.; Perriman, A. W.; Mann, S. *Nat. Commun.* **2014**, *5*, 5058.

(25) Brogan, A. P. S.; Sessions, R. B.; Perriman, A. W.; Mann, S. *J. Am. Chem. Soc.* **2014**, *136*, 16824−16831.

(26) Hunt, P. A.; Ashworth, C. R.; Matthews, R. P. *Chem. Soc. Rev.* **2015**, *44*, 1257−1288.

(27) Lees, J. G.; Miles, A. J.; Wien, F.; Wallace, B. A. *Bioinformatics* **2006**, *22*, 1955−1962.

(28) Whitmore, L.; Wallace, B. A. *Biopolymers* **2008**, *89*, 392−400.

(29) Whitmore, L.; Wallace, B. A. *Nucleic Acids Res.* **2004**, *32*, W668−W673.

(30) Cort, J. R.; Andersen, N. H. *Biochem. Biophys. Res. Commun.* **1997**, *233*, 687−691.

(31) Sönnichsen, F. D.; Van Eyk, J. E.; Hodges, R. S.; Sykes, B. D. *Biochemistry* **1992**, *31*, 8790−8798.

(32) D'Amico, M.; Raccosta, S.; Cannas, M.; Martorana, V.; Manno, M. *J. Phys. Chem. B* **2011**, *115*, 4078−4087.

(33) Ab Rani, M. A.; Brant, A.; Crowhurst, L.; Dolan, A.; Lui, M.; Hassan, N. H.; Hallett, J. P.; Hunt, P. A.; Niedermeyer, H.; Perez-Arlandis, J. M.; Schrems, M.; Welton, T.; Wilding, R. *Phys. Chem. Chem. Phys.* **2011**, *13*, 16831−16840.

(34) Cowan, D. A. *Comp. Biochem. Physiol.* **1997**, *118*, 429−438.

DOI: 10.1021/jacs.5b13425
J. Am. Chem. Soc. 2016, 138, 4494−4501

(35) Griebenow, K.; Klibanov, A. M. *J. Am. Chem. Soc.* **1996**, *118*, 11695−11700.
(36) Sharma, K. P.; Zhang, Y.; Thomas, M. R.; Brogan, A. P. S.; Perriman, A. W.; Mann, S. *J. Phys. Chem. B* **2014**, *118*, 11573−11580.
(37) Patil, A. J.; McGrath, N.; Barclay, J. E.; Evans, D. J.; Cölfen, H.; Manners, I.; Perriman, A. W.; Mann, S. *Adv. Mater.* **2012**, *24*, 4557−4563.

DOI: 10.1021/jacs.5b13425
J. Am. Chem. Soc. 2016, 138, 4494−4501